Supporting Information

Gan et al. 10.1073/pnas.1014963108

SI Text

Interference Pattern of the Plasmonic Mach–Zehnder Interferometer (MZI). The interference amplitude of the two surface plasmon polariton (SPP) waves on the two arms of the plasmonic MZI can be written as

$$E = a_1 \exp[i(k'_{SP1}L + \varphi_1)] + a_2 \exp[i(k'_{SP2}L + \varphi_2)], \quad \textbf{[S1]}$$

where

$$k'_{sp} = \frac{2\pi}{\lambda}\sqrt{\frac{\varepsilon'_m(\lambda)n^2}{\varepsilon'_m(\lambda)+n^2}} = \frac{2\pi}{\lambda}n_{\text{eff}}.$$

Consequently, the interference intensity could be described as

$$I = |E|^2 = a_1^2 + a_2^2 + 2a_1a_2\cos\left[\frac{2\pi L}{\lambda}(n_{\text{eff1}} - n_{\text{eff2}}) + \varphi_0\right]. \quad \textbf{[S2]}$$

One can see that the far-field interference pattern varies as $\cos[\frac{2\pi L}{\lambda}(n_{\text{eff1}} - n_{\text{eff2}}) + \varphi_0]$.

Finite Difference Time Domain (FDTD) Modeling of Interference Oscillations of the Plasmonic MZI with Various Groove Depths. The spectral interference patterns of the plasmonic MZI were simulated using a 2D FDTD model, and shown in Fig. S2. The thickness of the metal is 300 nm, and the wavelength range considered is 500–850 nm. The period and width of the grating structure are 520 and 150 nm, respectively. The distance between the two slits is 21 μm. One can see that, as the depth of the grooves increases, the interference patterns broaden gradually and the number of the interference periods per unit wavelength range gradually decrease, which is qualitatively consistent with the experimental results in Fig. 2*B*. In addition, as the depth increases, the interference oscillations disappear in a narrow wavelength range centered at approximately 550 nm as indicated by the arrows in Fig. S2. It is consistent with the formation of the bandgap shown in Fig. 1*B* [calculated by the rigorous coupled-wave analysis (RCWA) method]. The slight quantitative difference between the FDTD numerical modeling and the experimental results may originate from fabrication error and random surface roughness which is not fully incorporated into the FDTD simulations.

SPP Bandgap Engineering by Varying Grating Period and Depth. To further confirm the tunability of the SPP bandgap, a series of four structures was also fabricated, with grating period and groove width of approximately 635 and 200 nm, respectively. The milling times for three of the four structures are identical to three of those in Fig. 3*B*, with nominal depths of 5, 10, and 15 nm. The fourth structure is a slit doublet with no grooves. According to the RCWA modeling shown in Fig. S3*A*, a bandgap is formed in the 650–680 nm wavelength range (see the white arrows). This prediction is in good agreement with the measured interference patterns shown in Fig. S3*B*. The interference patterns between the wavelengths of 660 and 700 nm disappear as the groove depth increases (see the black arrows). There is a slight difference in wavelength between the measured and calculated bandgap, which may be attributed to surface roughness, fabrication imperfection, and uncertainty in experimental measurements. Nevertheless, these measurements provide clear evidence that the surface dispersion properties can be tuned by tailoring the dimensions of the nanopatterned surface.

Extraction of the Group Velocity of SPP Modes at the Nanopatterned Interface. The interferometric measurement is a straightforward approach to demonstrate reduced group velocity in nanophotonic structures (1). The group index of the signal arm of MZI could be approximately calculated using the following equation:

$$n_g^{\text{sig}}(\lambda) = \lambda_{\min}\lambda_{\max}/[2L(\lambda_{\min} - \lambda_{\max})] + n_g^{\text{ref}}(\lambda). \quad \textbf{[S3]}$$

Here L is the length of the signal arm. Based on this equation and measured data in Fig. 3*B*, values of v_g and n_{eff} of SPP modes can be extracted from the interference patterns, as shown in Fig. S4. The group index at the metal–air interface increases from 1.01–1.04 for a flat metal to 1.05–1.35 for nanopatterned surfaces in the spectral region of 600–800 nm. Fig. S4 also shows that the group index increases with increasing groove depth. We believe that these experimental data do demonstrate the broadband slowing of light in nanoengineered plasmonic structures.

This technique was successfully employed in slow light measurements in photonic crystal (PhC) waveguides published in 2005 (1). However, the plasmonic MZI structure employed in our experiment differs from PhC MZI structure in two important respects, making it more difficult to extract large values of the group index close to the band edge:

1. Because of intrinsic metal loss in visible domain, the loss for our plasmonic structures is significantly larger than that for PhC waveguide at telecom wavelengths (1). SPP modes with very small group velocities cannot propagate over long distances due to this loss. If one were to attempt to compensate for loss by using a smaller slit–slit distance, the period of the spectral interference pattern increases, leading to fewer interference oscillations in the spectral region employed in our experiments. As a result, large group indices at the band edge cannot be effectively extracted using this interference pattern technique.
2. For the PhC waveguide in ref. 1, the n_{eff} of the reference arm is smaller than that of the signal arm, so that when the band edge of the signal arm is approached, the difference in n_{eff} between the two arms increases. Therefore, more interference fringes are observed (see Fig. 2*A* in ref. 1). However, for our plasmonic structure, the reference arm at the metal–glass interface has a larger n_{eff} than the signal arm (i.e., the metal–air interface). Consequently, when a nanograting is introduced at the metal–air surface to increase n_{eff}, the difference between the two arms decreases (until n_{eff} of the nanopatterned surface exceeds that of the reference arm). As a result, fewer (rather than more) interference fringes are observed as the band edge is approached. From Fig. 3*B* and Fig. S2, one can see that the interference pattern at the lower frequency band edge is broadened (the period is increased).

In principle, larger group indices may be observed by redesigning the plasmonic MZI structure, by patterning the nanograting on the metal–glass interface. The reference arm, now the metal–air interface, has a smaller n_{eff} than the signal arm, and the difference increases with increasing grating depth, leading to higher frequency interference oscillations as the band edge is approached (similar to that observed for Vlasov's PhC waveguide; ref. 1). Preliminary modeling results in Fig. S5 show that the interference pattern for a grating structure with $L = 21$ μm, period = 700 nm, width = 360 nm, and depth = 10 nm oscillates more rapidly when the band edge is approached (around 750–760 nm, as indicated by the red circle). Using Eq. **S3**, one

estimates the group index to be 3.4–3.8 in the 755–763-nm wavelength region, which is close to the band edge. It should be noted that, as v_g decreases rapidly at the band-edge, the loss also increases significantly, making observation of higher frequency interference oscillations more difficult using this plasmonic MZI technique.

1. Vlasov YA, O'Boyle M, Hamann HF, McNab SJ (2005) Active control of slow light on a chip with photonic crystal waveguides. *Nature* 438:65–69.

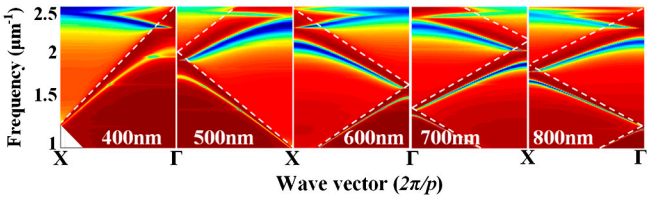

Fig. S1. Surface dispersion engineering of silver nanogroove arrays with various periods. The width and depth of the grooves are fixed at 150 and 30 nm, respectively, and the period is varied from 400 to 800 nm. One can see that the dispersion curves fall increasingly below the dashed light lines, and the frequency of the bandgap can be tuned over a broad spectral region by varying the grating period.

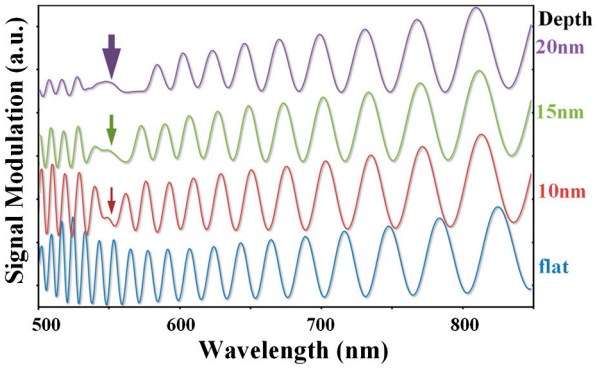

Fig. S2. Spectral interference patterns of the plasmonic MZI obtained using two-dimensional FDTD simulations. Nonuniform mesh sizes are employed in this modeling: The edge grid sizes are $\Delta x = 5$ nm and $\Delta z = 2$ nm, and body grid sizes are $\Delta x = 20$ nm and $\Delta z = 20$ nm.

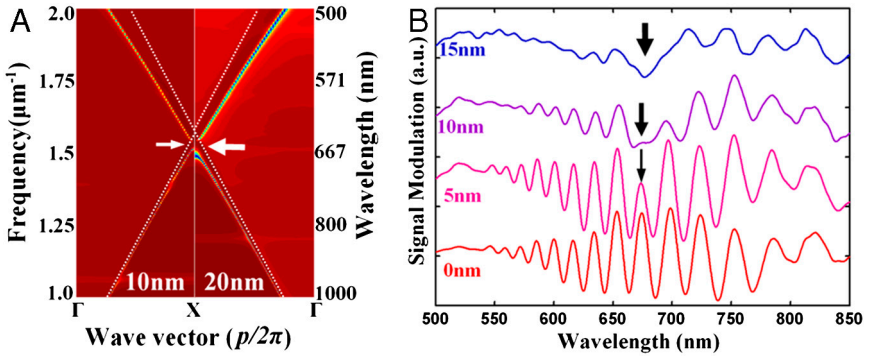

Fig. S3. (*A*) The dispersion diagram of a surface nanogroove array with depths of 10 and 15 nm calculated by the RCWA method. The period and width of the grooves are 630 and 150 nm, respectively. The dashed lines are light lines in free space. (*B*) Interference patterns from plasmonic MZIs: four doublet samples on a Ag film with groove depths of approximate 0, 5, 10, and 15 nm.

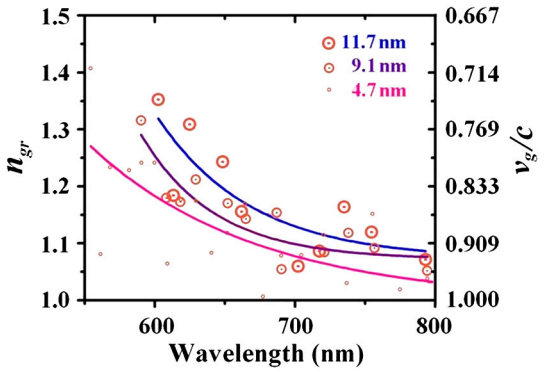

Fig. S4. Extraction of the group index and group velocity reduction from three interference patterns in Fig. 3*B* using Eq. **S3**. The solid lines are guides to the eye.

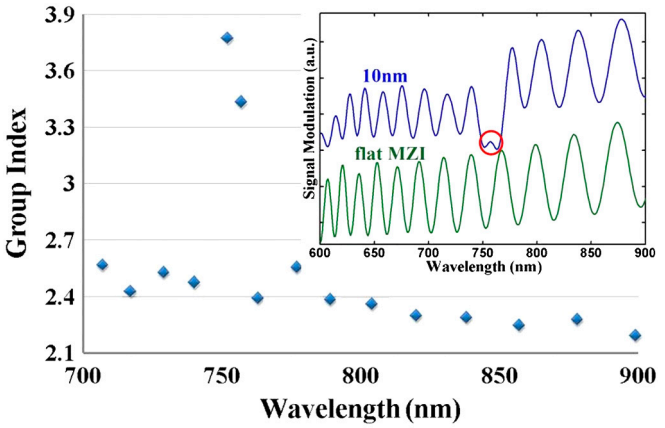

Fig. S5. Extraction of the group index from modeled interference pattern. (*Inset*) Interference patterns for plasmonic MZIs with a flat signal arm (lower curve) and a grating structure on the metal–glass interface with a parameters of $L = 21$ um, period $= 700$ nm, width $= 360$ nm, and depth $= 10$ nm (upper curve).